

A Study on the Ultimate Strength Analysis of Frame Structures by Idealized Structural Unit Method

J. K. Paik* and A. H. Lim**

理想化構造要素法에 의한 骨造構造物의 最終強度解析에 관한 研究
白点基* · 林華奎**

ABSTRACT

This paper presents an efficient and accurate method for nonlinear analysis of frame structures by idealized structural unit method. The main idea behind the present method is to minimize the cost of the computational effort by reducing the number of unknowns. An explicit form of the tangential elastic stiffness matrix of the element is derived by using updated Lagrangian approach. An ultimate limit state of the element is judged on the basis of the formation of a plastic hinge mechanism. The elasto-plastic stiffness matrix and the post-ultimate stiffness matrix of the element are formulated by plastic node method. A comparison between the present solution and the existing experimental and other numerical result for unit column member and simple frame structure is made. It is clear from the result of this study that the present method is very efficient and accurate because the computing time required is very small while giving the accurate solution.

1. Introduction

In order to carry out the safety assessment and reliable structural design of frame structures such as on/off-shore structure, it is essential to analyze the nonlinear behaviour of the structure associated with the geometric and material nonlinearity until it reaches the ultimate limit state as a whole.

Finite element method is one of the most powerful approaches to calculate the ultimate strength of these structures. However, because of the tremendous amount of computational effort, it is very difficult to apply it for the nonlinear analysis of large size structures, even if not impossible. As a countermeasure for this problem, Ueda et.al [1,2] have suggested the idealized structural unit method (ISUM). The efficiency of this method has been demonstrated for various types of steel structures such as offshore structures[3,4] and ship structures[1,5-7].

In this paper, ISUM is applied to the ultimate strength analysis of frame structures. For this purpose, an idealized structural element for beam-column member is developed. An explicit form of the tangential elastic stiffness matrix of the element is derived on the basis of the updated Lagrangian approach. The condition of ultimate limit state of the element is formulated considering the formation of a plastic hinge mechanism, in which the effect of damage in the form of local dent and overall deformation is taken into consideration. The elasto-plastic stiffness matrix and the element is derived by applying the plastic node method which is developed by Ueda et.al[8]. Also, the post-ultimate stiffness matrix of the element is formulated under a simple theoretical consideration.

The accuracy and efficiency of the present method is verified by comparing the present solution with the existing numerical and experimental results for unit column member, 2-D and 3-D frame structures.

2. Development of the Idealized Beam-Column Element

(1) Nodal Force and Nodal Displacement of the Element

In this paper, a large size beam-column member composing frame structures is chosen as an idealized beam-column element and the nodal point of the element is constructed at both ends. The behaviour of the element is expressed using six degrees of freedom at each nodal point, as shown in Fig. 1. Then, the incremental form of nodal force vector $\{\Delta R\}$ and nodal displacement vector $\{\Delta U\}$ reads

$$\{\Delta R\} = \{\Delta R_{x1}, \Delta R_{y1}, \Delta R_{z1}, \Delta M_{x1}, \Delta M_{y1}, \Delta M_{z1}, \Delta R_{xj}, \Delta R_{yj}, \Delta R_{zj}, \Delta M_{yj}, \Delta M_{zj}, \Delta M_{zj}\} \quad (1.a)$$

$$\{\Delta U\} = \{\Delta u_i, \Delta v_i, \Delta w_i, \Delta \theta_{xi}, \Delta \theta_{yi}, \Delta \theta_{zi}, \Delta u_j, \Delta v_j, \Delta w_j, \Delta \theta_{xj}, \Delta \theta_{yj}, \Delta \theta_{zj}\} \quad (1.b)$$

where, prefix Δ denotes the increment of each variable.

(2) Relationship Between Strain and Displacement

The strain-displacement relation in the longitudinal direction taking account of the large deformation effect is given by

$$\epsilon_x = u_{,x} - y \cdot v_{,xx} - z \cdot w_{,xx} + 1/2 \cdot v_{,x}^2 + 1/2 \cdot w_{,x}^2 \quad (2)$$

The incremental expression of Eq.(2) is emerged by the following matrix form[9]

$$\Delta \epsilon_x = ([B_p] - y[G_{vv}] - z[G_{ww}] + [C_v][G_v] + [C_w][G_w] + 1/2 \cdot [AC_v][G_v] + 1/2 \cdot [AC_w][G_w])\{\Delta U\} \quad (3)$$

* Member, Dept. of Naval Architecture, Pusan National University

** Student Member, Dept. of Naval Architecture, Pusan National University

where, $\Delta u_x = [B_p]\{\Delta U\}$, $\Delta v_x = [G_v]\{\Delta U\}$, $\Delta w_x = [G_w]\{\Delta U\}$, $\Delta v_{xx} = [G_{vv}]\{\Delta U\}$,
 $\Delta w_{xx} = [G_{ww}]\{\Delta U\}$, $v_x = [C_v]$, $w_x = [C_w]$

(3) Relationship between Stress and Strain

Neglecting the large deformation effect, the increment of the axial stress of the element is calculated by

$$\Delta \sigma_x = E [B_p] \{\Delta U\} \quad (4)$$

where, E : Young's modulus

(4) Derivation of the Tangential Elastic Stiffness Matrix

Applying the principle of virtual work, the following equilibrium equation should be satisfied.

$$\int_V \delta \Delta \epsilon_x^T (\sigma_x + \Delta \sigma_x) dv = \delta \{\Delta U\}^T (R + \Delta R) \quad (5)$$

where, the left hand side term of the above equation represents the strain energy stored during the action of the virtual strain increment and the right hand side indicates the external work done by the virtual displacement increment. Also, $\int_V (\cdot) dv$ denotes the integrating for the entire volume of the element and prefix δ denotes the virtual value.

Substituting Eq.(3) and Eq.(4) into Eq.(5) and neglecting the infinitesimal terms having higher order with regard to the increment, the elastic stiffness equation of the element in the local coordinate system is finally expressed by applying U. L. approach[9], that is,

$$\{\Delta R\} = [K]^* \{\Delta U\} \quad (6)$$

where, $[K]^* = [K_e] + [K_o]$: the tangential stiffness matrix of the element
 $[K_e]$: the small deformation stiffness matrix
 $[K_o]$: the initial stress stiffness matrix

Also, torsional stiffness of the element is given by using Saint-Venant linear theorem.

$$\begin{Bmatrix} \Delta M_{x1} \\ \Delta M_{x2} \end{Bmatrix} = \frac{GK}{L} \begin{bmatrix} 1 & -1 \\ -1 & 1 \end{bmatrix} \begin{Bmatrix} \Delta \theta_{x1} \\ \Delta \theta_{x2} \end{Bmatrix} \quad (7)$$

where, G : shearing modulus, K : twisting rigidity (= $I_y + I_z$)

(5) Displacement Function

The displacement function of the element is divided into two kinds of the shape, depending on the loading conditions, one for axial compression and the other for axial tension.

(a) Under the Axial Compression

When the dominant loading component is axial compression, buckling phenomenon will be occurred. In this case, the displacement function is then assumed by

$$u = a_1 + a_2 x \quad (8.a)$$

$$v = A_1 \cos k_z x + A_2 \sin k_z x + A_3 x + A_4 \quad (8.b)$$

$$w = B_1 \cos k_y x + B_2 \sin k_y x + B_3 x + B_4 \quad (8.c)$$

where, $k_z^2 = P/EI_z$, $k_y^2 = P/EI_y$

(b) Under the Axial Tension

In the same manner, the displacement function of the element subjected to axial tension reads

$$u = a_1 + a_2 x \quad (9.a)$$

$$v = A_1 \cosh k_z x + A_2 \sinh k_z x + A_3 x + A_4 \quad (9.b)$$

$$w = B_1 \cosh k_y x + B_2 \sinh k_y x + B_3 x + B_4 \quad (9.c)$$

where, $k_z^2 = P/EI_z$, $k_y^2 = P/EI_y$

(6) Criterion of the Ultimate Limit State

In this study, when a plastic hinge mechanism resulting from the occurrence of the global buckling or full plasticity is formed in the element, it is considered that the element reaches the ultimate limit state.

(a) Global Buckling

When the action of the axial compression is dominant, global buckling will take place which corresponds to the ultimate limit state, because the plastic collapse mechanism is immediately formed after global buckling has occurred.

If the axial stress is greater than Euler's buckling one, the element buckles, that is,

$$\Gamma_B = \sigma_a - \sigma_E \geq 0 \quad (10.a)$$

where, σ_a : axial compressive stress, σ_E : Euler's buckling stress

Also, Yoshiki et. al.[10] derived a simple formula for the estimation of the global buckling strength of the column taking account of the initial deflection. The present study employs Yoshiki's formula expressed by

$$\Gamma_B = \frac{\sigma_a}{\sigma_o} \left(1 + \frac{A a_o}{Z(1 - \sigma_a/\sigma_E)} \right) - 1 \geq 0 \quad (10.b)$$

where, σ_o : yield stress, Z : section modulus of the element, A : cross section area,

a_o : the magnitude of the initial deflection(global bending deformation)

Therefore, if any one condition of Eq.(10) is fulfilled, it is considered that the element reaches the global buckling strength.

(b) Full Plasticity

When the action of the bending moment is dominant or the magnitude of the initial deflection is relatively large, the global bending deformation increases from the beginning as the external force increases. In general, the largest bending moment is expected to be developed at both ends and/or in the midspan of the element. In this case, full plasticity at both ends and/or in the midspan of the element is formed when the internal forces satisfy the full plasticity condition. Thus, full plasticity is checked in the midspan as well as both ends in this study. Here, two kinds of the full plasticity condition are given whether or not the local dent is existed[11], that is,

(i) without local dent

$$\Gamma_P = \frac{M}{M_P} - \cos \frac{\pi}{2} \frac{P}{P_P} \geq 0 \quad (11.a)$$

(ii) with local dent

$$\Gamma_P = \frac{M}{M_P} - \cos \left[\frac{\pi}{2} \left(\frac{P}{P_P} - \frac{F_{dP}}{P_P} \right) + \frac{\alpha}{2} \right] + \frac{1}{2} \sin \alpha - \frac{\pi}{2} \frac{F_{dP}}{P_P} \left(\cos \alpha + \frac{\eta}{R} \right) \geq 0 \quad (11.b)$$

where, $P_P = 2\pi R t \sigma_y$: fully plastic axial force without a dent

$M_P = 4R^2 t \sigma_y$: fully plastic bending moment without a dent

$\alpha = \cos^{-1}(1 - 2D_d/D)$, $F_{dP} = 80 \cdot \sigma_y \cdot a \cdot t \cdot (\sqrt{4\eta^2 + t^2} - 2\eta)$, $\eta = (\sin \alpha a - \cos \alpha) \cdot D/2$

If Eq.(11) is satisfied at any cross-section, then the corresponding cross-section of the element becomes to be fully plastic condition.

(c) The Ultimate Limit State

As mentioned earlier, when a plastic hinge mechanism is formed, the element is considered to be collapsed. Thus, the condition of the ultimate limit state is described by the following two states:

(i) when the global buckling takes place

(ii) when the plastic hinge is formed at both ends as well as in the midspan of the element

(7) Elasto-Plastic Stiffness Matrix of the Element

If only one or two cross-section among both ends and midspan becomes to be plastic, the element exhibits the elasto-plastic behaviour since a plastic hinge mechanism is not formed yet.

For this state, the elasto-plastic stiffness matrix of the element which is derived by the plastic node method[8] is employed, that is,

$$\{ \Delta R \} = \left([K]^e - \frac{\sum [K]^e \{ \Phi_i \} \{ \Phi_i \}^T [K]^e}{\{ \Phi_i \}^T [K]^e \{ \Phi_i \}} \right) \{ \Delta U \} = [K]^P \{ \Delta U \} \quad (12)$$

where, $[K]^P$: the elasto-plastic stiffness matrix of the element.

(8) Post-Ultimate Stiffness Matrix of the Element

In the post-ultimate strength range, when the element is under the action of axial compression, a complicated unloading path occurs, which is dependent on the loading condition, dimensions and so on. In this case, the post-ultimate stiffness matrix of the element may be idealized by[12].

$$\{ \Delta R \} = [K]^u \{ \Delta U \} \quad (13)$$

where, $[K]^u$ is the post-ultimate stiffness matrix of the element and since the element carries only the membrane force, just axial components remain, in which other components become to be zero.

$$\begin{Bmatrix} \Delta R_{xi} \\ \Delta R_{xj} \end{Bmatrix} = \begin{bmatrix} \eta & -\eta \\ -\eta & \eta \end{bmatrix} \begin{Bmatrix} \Delta u_i \\ \Delta u_j \end{Bmatrix} \quad (14)$$

where, $\eta = -\frac{u_u u_o P_u}{u^2(u_o - u_u)}$, $u_o = 0.1L$, $u_u =$ axial displacement when $P=P_u$.

u : axial displacement

3. Numerical Results and Discussions

(1) Unit Column Member

Many researchers[13-18] conducted the ultimate strength test for damaged tubular members subjected to axial compression, in which simply supported end condition is considered. Here the accuracy of the present method is verified comparing with these experimental results. The damaged tubular member is modelled by only one idealized element in the present analysis.

A comparison between the present solution and the existing experimental results is made in Fig.2 and Fig.3. Since the COV for this comparison is less than 13%, it is considered the this present method gives the accurate solution.

(2) 2-D Frame Structures

Here, two types of 2-D frame structures are analyzed.

Fig. 4 indicates the ultimate test model for plane frame structure composing of tubular member, which was conducted by Paik et.al[9]. Test was performed for three cases which are denoted by P-IC, P-DC and P-RC model. The test specimen is modelled by using the idealized beam-column element in this study and the number of element and nodal point are 18 and 12, respectively. Rigid body is also modelled by the equivalent tubular element. Fig. 5 shows the load-displacement curve. It is observed that the present solution is in good agreement with the experimental result. The computing time required for this model was about 40 seconds by MIPS-M/120 computer.

Also, K-shaped 2-D frame model which was tested by Søreide et.al.[4] is analyzed, as shown in

Fig. 6. The number of the idealized element and nodal point used in the present analysis are 4 and 5, respectively. Fig. 7 shows the load-displacement curve. It is also clear that the present method gives an acceptable result in the pre- and post- ultimate strength range.

(3) 3-D Frame Structures

Fig. 8 indicates the ultimate strength test model for spatial frame structure[9]. The number of the idealized element and nodal point used in the present analysis are 56 and 28, respectively. Fig. 9 shows the load-displacement curve. It is observed that the present method gives an acceptable result comparing with the experimental result. The computing time required for this model was about 15 minutes by MIPS-1/20 computer.

Also, other model which was analyzed by Søreide et.al.[4] is calculated, as shown in Fig. 10. The number of the idealized element and nodal point used in this present analysis are 28 and 13, respectively. The load-displacement curves are compared in Fig. 11. The present solution corresponds to Søreide's numerical result very well.

4. Conclusion

In this paper, an idealized beam-column element was developed to analyze the ultimate strength of the frame structure. Comparing the present solution with the existing numerical and experimental results for unit tubular column, 2-D and 3-D frame structures, it is observed that the present method gives an accurate solution and is very efficient since the computing time required is very small.

REFERENCE

- [1] Ueda, Y. and Rashed, S. M. H., "The Idealized Structural Unit Method and it's Application to Deep girder Structures", Computer and Structures, Vol.18, No.2, 1984.
- [2] Ueda, Y. and Rashed, S. M. H., "Advances in the Application of Idealized Structural Unit Method", Int. Conf. of Advances in Marine Structures, ARE, Dunfermline, Scotland, 1991(to be appeared).
- [3] Ueda, Y. and Rashed, S. M. H., "Behaviour of Damaged Tubular Members in Offshore Structures", OMAE, pp.528-536. 1985.
- [4] Søreide, T. H. and Amdahl, J., "Collapse Analysis of Framed Offshore Structures", OTC5302, 1986.
- [5] Ueda, Y. et.al., "Ultimate Strength Analysis of Double Bottom Structures in Stranding Conditions", PRADS'87, Trondheim, Norway, 1987.
- [6] Paik, J. K., "Ultimate Strength Analysis of Ship Structures by Idealized Structural Unit Method" Dr. Dissertation, Osaka University, 1987.
- [7] Paik, J. K. and Lee, D. H., "Ultimate Longitudinal Strength-Based Safety and Reliability Assessment of Ship's Hull Girder", J. of SNAJ, Vol.168, 1990.
- [8] Ueda, Y. and Yao, T., "The Plastic Node Method : A New Method of Plastic Analysis ", Computer Methods in Applied Mechanics and Engineering, Vol. 34, Nos. 1-3, pp.1089-1104, 1982.
- [9] Paik, J. K. and Shin, B. C., "A Study on the Ultimate Strength Analysis of Damaged Tubular Members", J. of SNAJ, Vol.27, No.1, pp.24-34., 1990.
- [10] Yoshiki, K., et. al., "Elastic Stability", Kyoritsu Publishing Co., 1965.
- [11] Yao, T, Taby, J. and Moan, T., "Ultimate Strength and Post-Ultimate Strength Behaviour of Damaged Tubular Members in Offshore Structures", OMAE'86, pp.301-308, 1986.
- [12] Paik, J. K. and Shin, B. C., "Theoretical and Experimental Study for the Progressive Collapse Analysis of Tubular Offshore Structures", PACOMS'90, Vol.3, pp.367-374, 1990.
- [13] Rashed, S. M. H., "Ultimate Strength and Post-Ultimate Strength Behaviour of Damaged Tubular Members", Report SK/R52, Division of Marine Structures, Norwegian Institute of Technology, 1980.
- [14] Smith, C. S., Kirwood, W., and Swan, J. W., "Buckling Strength and Post-Collapse Behaviour of Tubular Members Including Damage Effects", Proc. 2nd Int. Conf. on Behaviour of Offshore Structures (BOSS 79), London, pp.303-326, 1979.
- [15] Smith, C. S., Somerville, W. L. and Swan, J. W., "Residual Strength and Stiffness of Damaged Steel Bracing Members", OTC 3981, pp.273-282, 1981.
- [16] Smith, C. S., "Assessment of Damage in Offshore Steel Platforms", Proc. of Int. Conf. on Marine Safety, pp.279-307, 1983.
- [17] Smith, C. S., "Residual Strength of Tubulars Containing Combined Bending and Dent Damage", Proc. Offshore Operations Sympos., 9th Energy-Sources Technology Conf., 1986.
- [18] Taby, J., Moan, T. and Rashed, S. M. H., "Theoretical and Experimental Study of the Behaviour of Damaged Tubular Members in Offshore Structures", Norwegian Maritime Research, Vol. 9, No.2, pp.26-33, 1981.

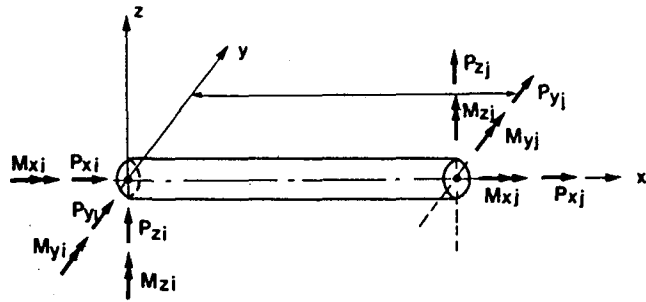


Fig. 1 The idealized beam-column element

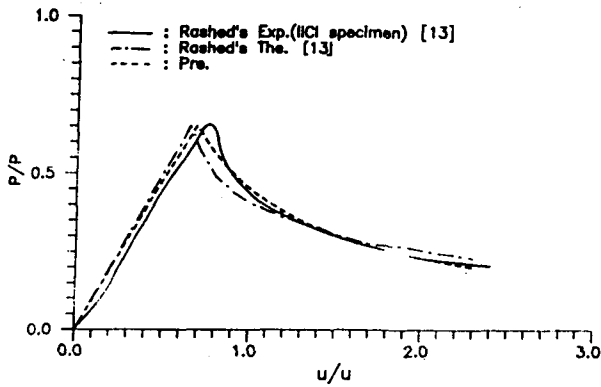


Fig. 2 The load-shortening curve for damaged tubular member subjected to axial compression

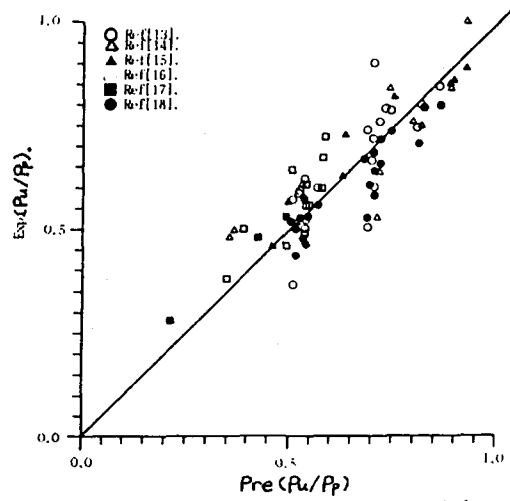


Fig. 3 Comparison of the ultimate strength between present solutions and experimental results

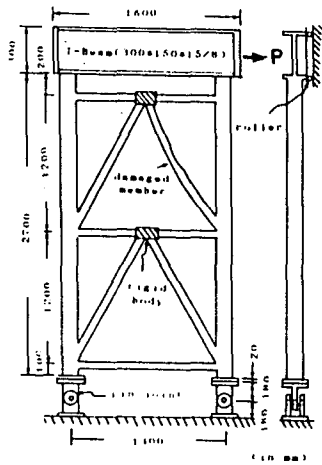


Fig. 4 Configuration of Paik's 2-D frame structure model[9]

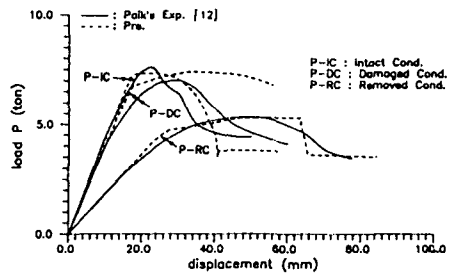


Fig. 5 The load-displacement curve for Paik's 2-D frame structure model

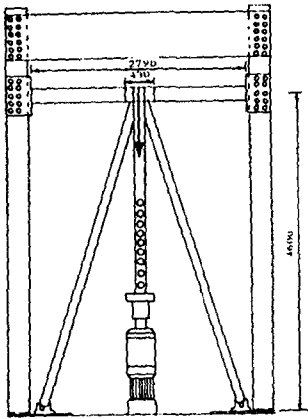


Fig. 6 Configuration of Sørveide's K-shaped frame structure model[4]

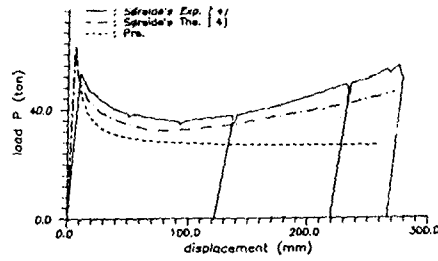


Fig. 7 The load-displacement curve for Sørveide's K-shaped frame structure model

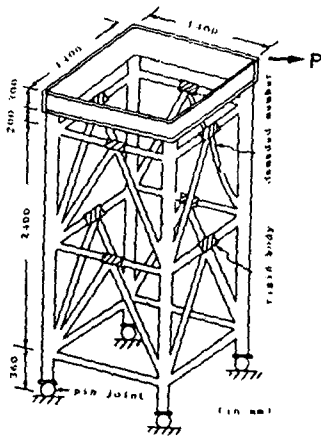


Fig. 8 Configuration of Paik's 3-D frame structure model[9]

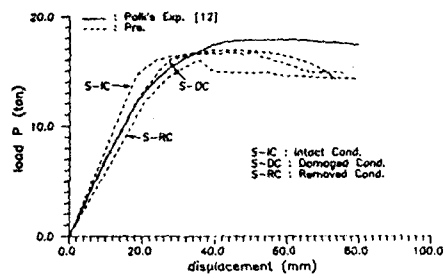


Fig. 9 The load-displacement curve for Paik's 3-D frame structure model

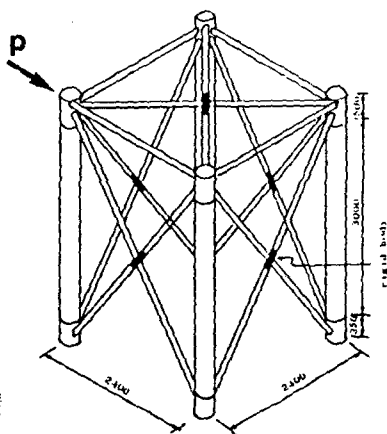


Fig. 10 Configuration of Sørveide's 3-D frame structure model

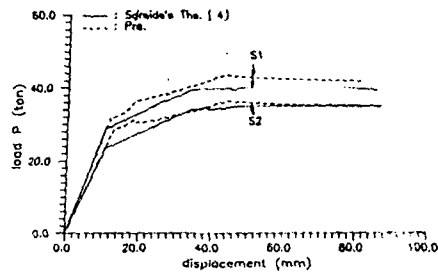


Fig. 11 The load-displacement curve for Sørveide's 3-D frame structure model